

Numerical modeling of Concrete microstructure with poly-mineral Aggregate using image-based Analysis

Hyeong-Tae Kim^a, Kyoungsoo Park^{a*}

^aDepartment of Civil and Environmental Engineering, Yonsei University, 50 Yonsei-ro, Seodaemun-gu, Seoul 120-749, Republic of Korea

*Corresponding author: k-park@yonsei.ac.kr

***Keywords : Concrete microstructure, Rock-forming mineral, Image-based Analysis, Neutron irradiation. Radiation Induced Volume Expansion(RIVE).**

1. Introduction

The deterioration due to radiation on the concrete is a key points on in nuclear power plants (NPPs) as different from that of other structures. The performance degradation of concrete exposed to long-term neutrons has been demonstrated in previous researches [1 2], and the Radiation Induced Volume Expansion(RIVE) of the aggregate is an important factor[3]. In generally, natural rock aggregate is composed of poly-minerals, and the maximum expansion ratio of RIVE is according to each mineral. In this study, a numerical simulation for the actual concrete microstructure with poly-mineral aggregate is proposed. It included microstructure reconstruction for the image processing, and image-based Analysis.

2. Concrete Microstructure Reconstruction with poly-mineral Aggregate

A concrete specimen has the size of 20 × 20 × 80 mm. Fine aggregate is used siliceous natural sand, less than 2mm size. Coarse aggregate is used crushed gabbro rock is used, size from 2mm to 8mm. The composition of rock forming mineral to the sand was mainly quartz, and gabbro aggregate was mainly plagioclases, hornblende, and pyroxene. Digital Images were obtained using X-ray and neutron CT in Fig 1. X-ray tomography were taken at the Korea Institute of Civil Engineering and Building Technology, The thermal neutron tomography were taken at the RAD facility of the Centre for Energy Research, Hungary. Pixel size is 13um and 43um for each X-ray and neutron CT.

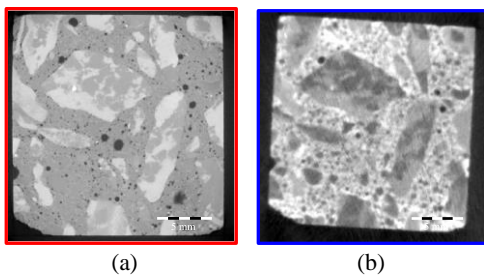


Fig. 1. Computer tomography image for the (a) X-ray, and (b) Neutron.

Concrete microstructure is reconstructed six components: aggregate (quartz, plagioclase, pyroxene, hornblende), paste and void. Image segmentation for the X-ray and neutron CT for the aggregate, paste, and void was using Otsu method. Image registration for the segmented image for the X-ray and neutron into three material phases are using the position of the void [4]. The region for the reconstructed microstructure is classified based on the material phases on the each X-ray and neutron images which shown in Figure 2. Void (yellow) is an area with a low gray value based on high-resolution X-rays. Paste (gray) is relatively low in density except for pores and contains hydrogen, so it is based on the high gray value area in the middle neutron in X-rays. Hornblende (red) can be classified only in X-rays, and both images have high gray values due to high density and hydrogen. Pyroxene (black) is classified as redundant in X-ray and neutron. It is dense and has no hydrogen, so it is high in X-ray and medium gray value in neutron. Plagioclase (green) and quartz (blue) is distinguished only in neutron, and since there is no hydrogen at relatively low density, it is in the middle gray value region even in middle neutron in X-ray. These two minerals are classified with particle size in 2mm boundary between fine and coarse aggregate

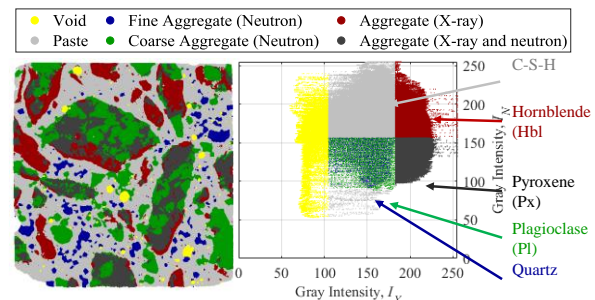


Fig. 2. Reconstructed concrete microstructure using the complementarity of x-ray and neutron CT

3. Image based Virtual Element Method

To efficiently analyze complex microstructure like concrete, the image-based virtual element method (VEM) is presented. Polygonal elements have been widely utilized because of the flexibility on the element shape. While the integration using the non-polynomial

shape functions on arbitrarily polygonal elements is computationally challenging. To consistently handle the non-simply elements, the VEM was proposed by implicitly defining shape functions of polygonal elements in conjunction with the projection operators.

A microstructure mesh for the polygonal elements is directly obtained from the reconstructed microstructure. It has four step. 1) Find node coordinate based on the pixel information on the reconstructed image which has certain number of material phases in Fig 3 (a), 2) Find edges located between pixels which has different materials, and necessary to record the material types on two material types in Fig 3. (b). 3) In order to improve the computational cost, coarsening is performed on the classified nodes and edges. Selects nodes separated by a specified length along the edge and create a new edges in Fig 3 (c). 4) Finally, For the remaining materials except for void, the edge list is classified based on the material type stored information at 3) for each material. and create the elements according to these edge set in Fig 3 (d).

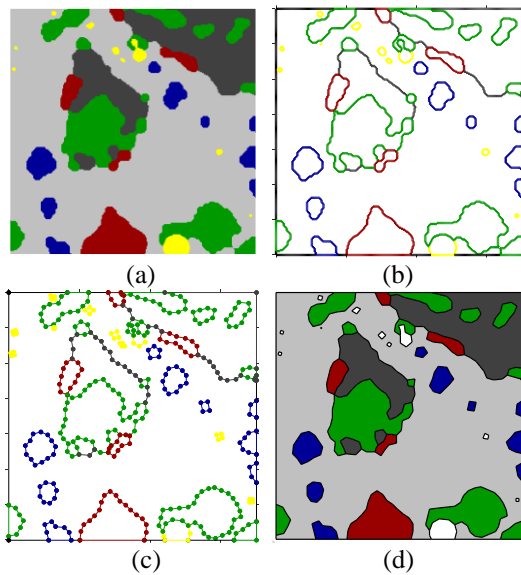


Fig. 3. Schematics of the polygonal mesh generation with a: (a) microstructure mesh, (b) homogeneous mesh, and (c) integration of homogeneous and microstructure mesh.

3. Numerical Examples

3.1 Material Properties

The elastic moduli of the aggregate and paste are selected as 92.0 GPa, 97.9 GPa, 84.1 GPa, 101.5 GPa, and 20 GPa, respectively; the Poisson's ratio of the aggregate and paste are 0.282, 0.338, 0.099, 0.264, and 0.2, respectively. The RIVE for the each rock-forming mineral is approximated for the fitting equation as [5] based on the experiment data in Fig 4. The RIVE of the paste under neutron irradiation can be negligible compared to the aggregate.

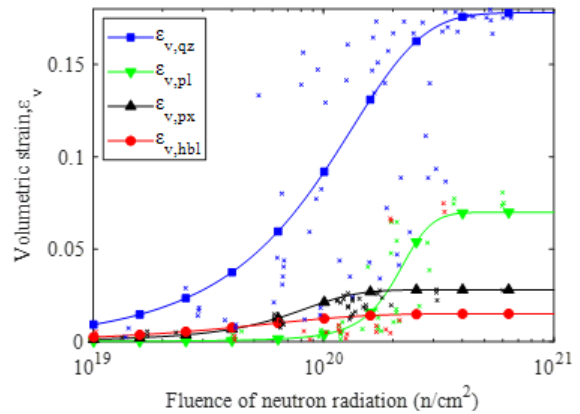


Fig. 4. Zubov and Ivanov's sigmoidal model for the radiation induced volume expansion of rock-forming minerals(Le pape et al. 2018) in gabbro aggregate based on the experiment data.

3.2 Uniaxial tension test

Concrete microstructure is the rectangular domain, as shown in Fig. 5. Image size is 1,232 pixel \times 1,232 pixel. Gabbro aggregate is classified into four types of rock-forming minerals, which are plagioclase (green), pyroxene (black), quartz (blue), and hornblende (red), respectively. Fluence of neutron radiation level applied from un-irradiation to 2×10^{21} n/cm².

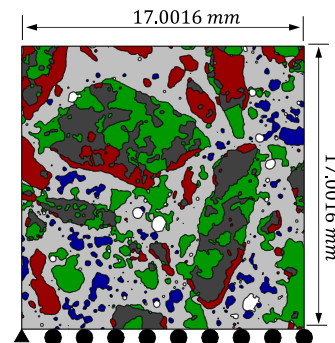


Fig. 5. Geometry and boundary conditions of the concrete microstructure on the RIVE of aggregate.

Fig 6. demonstrate the change in the macroscopic volume of the entire concrete according to the RIVE of the rock forming mineral according to the neutron irradiation. The volume change of concrete is calculated based on the total area of the deformed element and the initial area. Cross sections for the concrete microstructure for the images on horizontal slides of three difference location on the specimen. The numerical results demonstrate that as the fluence of neutron radiation increases, the entire volume of concrete increases, which is matched with the region of the experimental results.

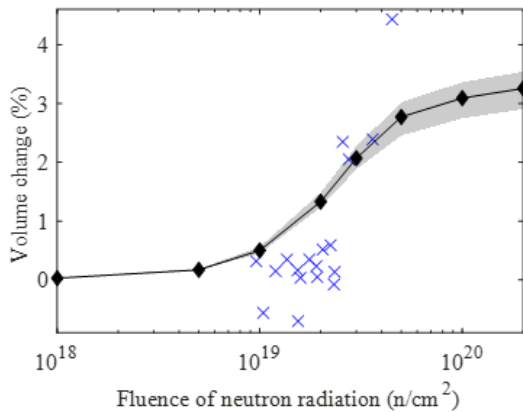


Fig. 6. Concrete volume change according to the flocunce of neutron radiation..

4. Conclusion

The complementarity of X-ray and Neutron CT, the concrete microstructure is effectively reconstructed and the rock forming minerals of the aggregate are distinguished. The VEM is used to analyze the discretized concrete microstructure for arbitrary polygonal elements. Microstructure mesh based on the image, more efficient discretization of complex microstructures is performed. The concrete microstructure analysis under RIVE of the aggregate was performed well using the proposed process. The proposed image-based VEM provides a result efficiently, and well-math with the distribution of experimental data.

ACKNOWLEDGEMENTS

This work was supported by the National Research Foundation of Korea (NRF) grant funded by the Korea government (Ministry of Science and ICT) (No. RS-2022-0014450).

REFERENCES

- [1] K. G. Field, I. Remec, and Y. Le Pape, Radiation effects in concrete for nuclear power plants – Part I: Quantification of radiation exposure and radiation effects, *Nuclear Engineering and Design*, Vol.282, p. 126-143, 2015.
- [2] K. Willam, Y. Xi, and D. Naus, A review of the effects of radiation on microstructure and properties of concrete used in nuclear power plants, U.S. Nuclear Regulatory Commission, NUREG/CR-7171, 2013.
- [3] T. M. Rosseel, I. Maruyama, Y. Le Pape, O. Kontani, A. B. Giorla, I. Remec, J. J. Wall, M. Sircar, C. Andrade, and M. Ordonez, Review of the current state of knowledge on the effects of radiation on concrete, *Journal of Advanced Concrete Technology*, Vol.14(7), p.368-383, 2016.
- [4] H. T. Kim, D. F. Tiana Razakamandimby R, V. Szilágyi, Z. Kis, L. Szentmiklósi, M. A. Glinicki, and K. Park, Reconstruction of concrete microstructure using complementarity of X-ray and neutron tomography. *Cement and Concrete Research*, Vol.148, p.106540, 2021.

- [5] Y. Le Pape, M. H. Alsaïd, and A. B. Giorla, Rock-forming minerals radiation-induced volumetric expansion-revisiting literature data, *Journal of Advanced Concrete Technology*, Vol.16(5), p.191-209, 2018.